

## Studies of Polyvinyl Alcohol/Alkali Lignin/Silica Composite Foam Material (PLCFM)

Huachao Luo,<sup>a</sup> Jing Lu,<sup>a</sup> Shixue Ren,<sup>a,b,\*</sup> Guizhen Fang,<sup>a,b</sup> and Guiquan Jiang<sup>c</sup>

This study investigates methods for improving the heat resistance of polyvinyl alcohol/alkali lignin foam material (PLFM). Tetraethoxysilane (TEOS) was used as a precursor to prepare PLCFM by a sol-gel method. The PLCFM, prepared with different levels of TEOS, was characterized by Fourier Transform Infrared spectrometry (FTIR), Differential Scanning Calorimetry (DSC), and Thermogravimetric Analysis (TGA). The results indicated that the addition of silica notably improved the heat resistance properties and the initial decomposition temperature of the foam and exhibited good biocompatibility with the polyvinyl alcohol (PVOH) and alkali lignin. The melting temperature of the PLCFM also increased significantly. It reached 268 °C when the silica content was 10%, which was 110 °C higher than that of PLFM. The mechanical properties were also improved to 27.42 MPa.

*Keywords:* Polyvinyl alcohol; Alkali lignin; Functional composite; Thermal properties; Sol-gel methods

*Contact information:* a: College of Material Science and Technology, Northeast Forestry University, Harbin, 150040, P. R. China; b: Key Laboratory of Bio-based Material Science and Technology (Northeast Forestry University), Ministry of Education, Harbin, 150040, P.R. China; c: College of Forestry, Beihua University, Jilin, 132013, P. R. China; \*Corresponding author: renshixue@nefu.edu.cn

### INTRODUCTION

Lignin is an abundant natural polymer with a complex structure, but only 6% of the lignin in pulp black liquor is utilized as raw material to synthesize high performance materials. Lignin consists of an amorphous three-dimensional macromolecule held together by C-C and ether bonds. Its molecular structure consists of many hydroxyl groups, which allows lignin to be used as a polyol, and at the same time its phenylpropanoid structure also has certain desirable mechanical properties (Lewis and Yamamoto 1990; Abdul *et al.* 2011). Alkali lignin, the main by-product of the pulping and papermaking industries, has excellent performance characteristics (Malutan *et al.* 2008), such as high surface activity, non-toxicity, heat resistant weathering, and anti-ultraviolet properties, which has led to its extensive study (Kabir *et al.* 2006; Pan and Saddler 2013). Polyvinyl alcohol foam has been widely applied as a thermal insulation material due to the excellent performance characteristics, such as strong water absorption capacity, good softness, a highly porous structure, wear resistance and weather resistance, and finally chemical stability and biocompatibility (Rachipudi *et al.* 2011; Li *et al.* 2012). Thus, its poor mechanical properties, high cost, and resistance to degradation have hampered its application.

In preliminary work alkali lignin was grafted into polyvinyl alcohol foam material and prepared PLFM by cross-linking and blending (Luo *et al.* 2015). The resulting PLFM exhibited greatly enhanced mechanical properties; the cost was also greatly reduced. However, the PLFM exhibited a lower degree of acetalization, of about 60% to 70%, and

its molecular structure contained a large amount of unreacted hydroxyl groups, which greatly contributed to its tendency to absorb moisture. At the same time, the PLFM was easily degraded, and its thermal stability was also worse under high temperature, which would severely limit its application in a relatively high-temperature environment. During the experiment the degree of acetalization of the PLFM was increased by increasing the acetal reaction time, the amount of formaldehyde, and stirring speed and making a few other changes. The methods applied had notably improved the heat resistance properties of PLFM, but at an increased cost; meanwhile, the recovery of the formaldehyde was more difficult, which resulted in greater environmental concerns.

Silica is not only the raw material important to the manufacture of glass and optical instruments, but it is the raw material that is essential for refractory materials. The researchers, Hsiue and Salinas (Hsiue *et al.* 2000; Salinas *et al.* 2007), applied silica to PS and PDMS, which greatly improved the biological compatibility and thermal stability of the materials. However, because silicon dioxide is difficult to react because of its stable chemical properties, the silica precursor TEOS was used as the raw material in the modification of PLFM by the products of hydrolysis in an acidic environment (Corradini *et al.* 1999). Using sol-gel technology (Brinker *et al.* 1984; Schmidt *et al.* 1984; Wu *et al.* 2006), a PLCFM was prepared by means of combining organic materials with inorganic material through a simple process (Wouters *et al.* 2004; de Oliveira *et al.* 2008). The PLCFM with the excellent performance of organic materials and inorganic materials, such as wear resistance, heat resistance, and so on. In this study, FTIR was used on the PLCFM in order to determine its structure as part of an attempt to obtain more details regarding the relationship between the silica content and the heat resistance properties of the PLFM. The thermal degradation and thermal stability of the PLCFM were studied by means of TGA and DSC. Finally, the effects of silica content on the properties were determined for the PLCFM.

## EXPERIMENTAL

### Materials

PVA (2488) (88% degree of hydrolysis; 2400 degree of polymerization) was obtained from Shandong Chemical Plant. Industrial alkali lignin was purchased from Shandong Paper Mill. Sodium bicarbonate, formaldehyde, TEOS, sulphuric acid, all of analytical reagent grade, were acquired from Beijing Chemical Reagent Factory, China.

### Methods

#### *Preparation of PLCFM*

PVA (5 g) and water (95 mL) were fed into a 500-mL three-neck flask fitted with a stirrer, a thermometer, and a reflux condenser. The mixture of alkali lignin (1.5 g) and sodium bicarbonate (4.0%, mass fraction) was added to the above reactive system, stirring was applied for 5 min, and then TEOS and HCHO (4 mL) were added. The reaction temperature was kept at 80 °C, and the reacting solution was kept under reflux for 2 h. After the stirring, sulphuric acid (0.02 mol) was added, and the solution was shifted into a mold and cross-linked at 120 °C over the course of 2 h. After the reaction was completed, it was followed by washing and solidification, and a novel PVA/alkali lignin/silica composite foam material (PLCFM) was obtained.

### *Mechanical performance*

The tensile test was performed in accordance with the standard method GB130022-91 (1991). The thickness of the films was measured using an electronic digital readout micrometer with an accuracy at 0.001 mm. Rectangular samples, 150 mm in length and 20 mm in width, were cut at a drawing speed of 50 mm/min. The test was performed by an LDX-200 Intelligent Electronic Universal Testing Machine, Beijing Landmark Packing Material Co., Ltd. At least five samples from each PLCFM were evaluated (Su *et al.* 2013).

### *Apparent density*

The apparent density test was performed in accordance with the standard method GB/T6343-2009/ISO 845:2006 (2006). The weight of the rectangular sections (100 mm in length, 100 mm in width, and 10 mm in thickness) was determined using an analytical balance (G 0.0001 g). The weight and the volume of each section were then used to calculate the density. At least five samples from each PLCFM were evaluated. The apparent density was calculated as,

$$\rho = m/V \quad (1)$$

where  $\rho$  is the apparent density of PLCFM,  $m$  is the quality, and  $V$  is the volume.

### *Absorption properties*

The absorption properties test was performed in accordance with the standard method GB/T8810-2005 (2005). Rectangular samples were cut to measure 50 mm in length and 50 mm in width. The mass ( $m_1$ ) and volume ( $V_0$ ) were weighed accurately, and the surface weight of a wetted net cage was noted as  $m_2$ . The foam material was loaded into the wetted net cage, then placed into water and soaked for 24 h. Finally, the component denoted as  $m_3$  was weighed. At least five samples from each version of the foam material were evaluated. The absorption rate was calculated as,

$$W = [m_3 + V_1 \times \rho - (m_1 + m_2 + V_c \times \rho)] / (V_0 \rho) \times 100\% \quad (2)$$

where  $W$  is the absorption rate,  $m_1$  is the sample mass,  $m_2$  is the mass of the wetted net cage,  $m_3$  is the mass of the sample and the net cage after the water had been absorbed,  $V_0$  is the sample volume,  $V_c$  is the sample volume of the surface bubble, and  $\rho$  is density of water.

### *FT-IR spectrometer*

PLCFM was mixed with a sample of KBr in a ratio of 1:100, and the mixture was formed into a pellet. All FTIR measurements were performed using a Magna-IR560 spectrometer, Thermos Nicolet Corporation (USA). Each sample was scanned 16 times at a resolution setting of 2  $\text{cm}^{-1}$  and averaged to produce each spectrum.

### *Scanning electron microscopy (SEM) and Energy Dispersive Spectroscopy (EDS)*

The surface morphology of PLCFM was examined using a Quanta200 Electron Microscope after it was dried to constant weight at 50 °C. PLCFM was gold-coated prior to microscopic observation.

### Thermal analysis

The thermal analysis of the PLCFM was conducted using a Q20 DSC and Q50 TGA, America TA Equipment Co. Ltd. All differential scanning calorimeter (DSC) tests were carried out under flowing nitrogen (10 mL/min) at a linear heating rate of 10 °C/min, ranging from room temperature to 300 °C. All thermogravimetry analysis (TGA) tests were carried out at a linear heating rate of 10 °C/min under pure nitrogen. The temperature ranged from room temperature to 800 °C. All thermal degradation data were obtained from TG and DTG curves.

## RESULTS AND DISCUSSION

### Mechanical Performance

Figure 1 gives the mechanical performance of the PLCFM curves with different silica contents. Without silica, the tensile strength and rupture elongation of the foam material were 25.91 MPa and 7.5%, respectively. The PVA, alkali lignin, and silica have good biocompatibility, and the addition of the silica greatly lengthened the molecular chain of PLCFM, which contributed to the formation of an interpenetrating structural network and greatly increased the tensile strength of the PLCFM. Later in the experiment, after the high-temperature curing, the toughness and tensile strength of the PLCFM increased, but this was not conducive to the ductility, and accordingly the rupture elongation decreased with the addition of the silica.

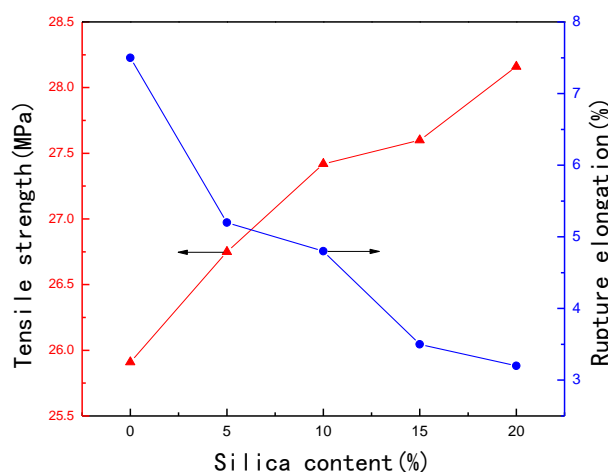
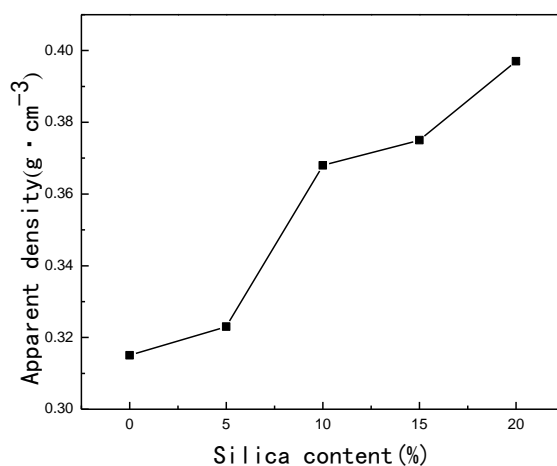


Fig. 1. Effect of silica content on mechanical performance of PLCFM

### Apparent Density

Figure 2 illustrates the effects of silica content on the apparent density of PLCFM. When the TEOS was integrated into the mixture, the apparent density of the PLCFM increased because of the growth of the molecular chain, the incassation of the foam skeleton, and the thickening of the cell wall. At the same time, during the high-temperature treatment the water volatilization caused volume deformation, which worsened with the length of the molecular chain, and which ultimately caused a decrease in the apparent density. When these two factors interacted, the apparent density decreased as the silica content increased.



**Fig. 2.** Effect of silica content on apparent density of PLCFM

### Absorption Properties

The effects of silica content on the absorption properties of the PLCFM are shown in Fig. 3. TEOS contributed to strong water-resistance performance and was able to hydrolyze to produce hydroxyl groups, which could react in the PLFM and reduce the hydroxyl content in the molecules. The surface pores of the foam were occupied by water-resistant silica, which hindered contact between the absorbent group and the water molecules. Meanwhile, the increase in apparent density and the reduction in pore structure between the molecules were not conducive to the water absorption. Thus, the water absorbency declined with the increase in silica content.

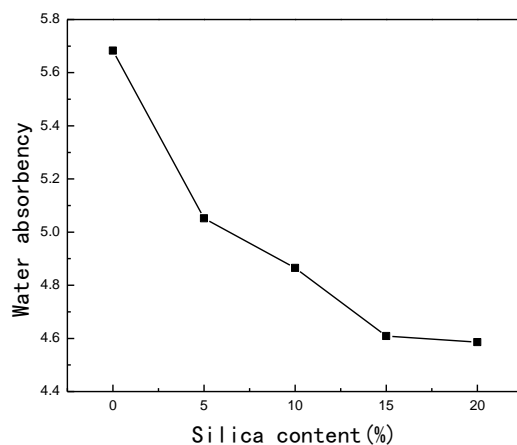


**Fig. 3.** The effects of silica content on the absorption properties of PLCFM

### Effect of Silica on the Structure of PLCFM

The mechanism behind the acid-catalyzed hydrolysis of TEOS is presented in Fig. 4. (I). The acid-catalytic hydrolysis of TEOS is a proton electric mechanism; its hydrolysis of all ethoxy groups is selective (Malay *et al.* 2013). Once one ethoxy group hydrolyzed, the ethylene oxide hydrolysis rate of the others was relatively slow. Along with the hydrolysis and polycondensation reaction, TEOS originally polymerized the three-

dimensional network structure, easily forming a silica sol network structure, and ultimately contributing to the formation of colloidal silica (Zaharescu *et al.* 2003), as presented in Fig. 4. (II). Hydrolysis condensation only occurs with a small proportion of hydroxyl groups because of the selectivity of acid-catalyzed TEOS. Better dispersion of primary products contributed to higher condensation reaction activity of the PLFM, which allowed the silica to graft easily onto the PLFM macromolecules. The above reactions coincided explosively with the acetal reaction, such that along with the basic TEOS hydrolysis condensation polymerization reaction, the acetalization of PVA with alkali lignin, and the additional condensation reaction between them, a highly cross-linked interpenetrating network structure was established. The condensation reaction mechanisms of the PLFM and TEOS hydrolysis are presented in Fig. 4. (III).

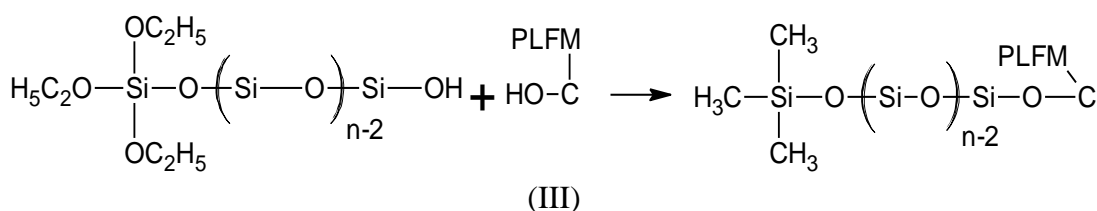
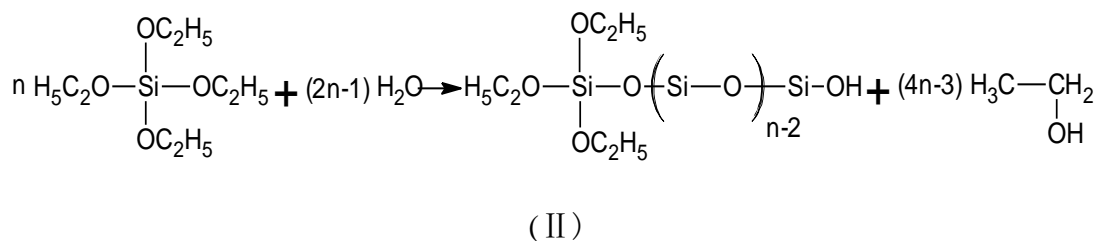
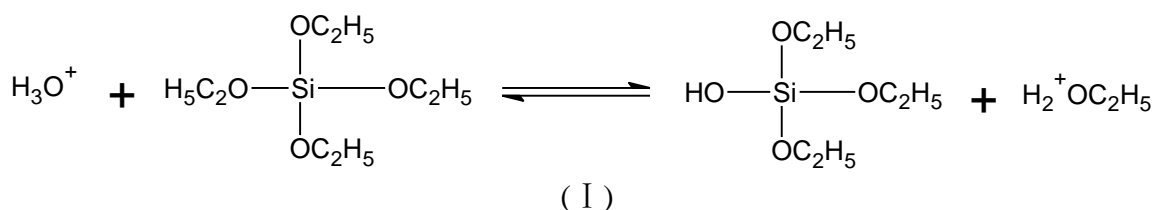


**Fig. 4.** Condensation reaction of PLFM and TEOS hydrolysis

FTIR spectra for PLCFM are presented in Fig. 5. For PLFM, the O-H stretching vibration absorption peak of hydroxyl groups is found at  $3440 \text{ cm}^{-1}$ , the double alcohol vibration absorption peak at  $1700$  to  $1720 \text{ cm}^{-1}$ , the stretching vibration absorption peak of the secondary alcohol at  $1069 \text{ cm}^{-1}$ , and the C-O-C-O-C stretching vibration peak at  $1242$  and  $1018 \text{ cm}^{-1}$ . The spectrum of PLCFM was similar to that of PLFM, except that the increase in the intensity of the absorption peak at  $1180$  to  $1080 \text{ cm}^{-1}$ , which was mostly due to C-O-Si and Si-O-Si, appeared during the reaction process (Anbarasan *et al.* 2010). At the same time, the primary alcohol shock absorption peak at  $1012 \text{ cm}^{-1}$  was weakened because of the increased primary alcohol content in the reaction. The above research results demonstrated that the condensation products of the TEOS hydrolysis successfully linked with the PLFM macromolecules.

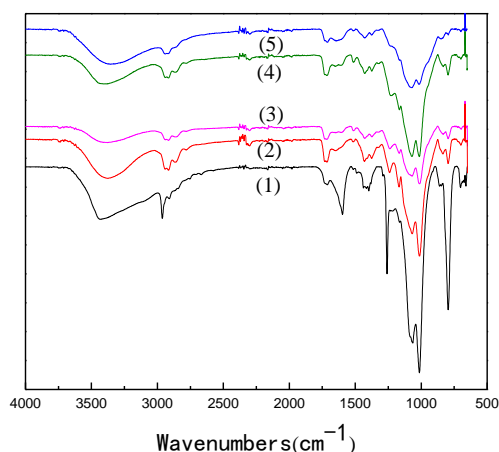


**Fig. 5.** FTIR spectra for PLCFM: SiO<sub>2</sub> contents (%) (1)-0; (2)-5; (3)-10; (4)-15; (5)-20

### SEM-EDS

In the process of acetal or hemiacetal, the stress caused by water evaporation destroyed the structure of the PLCFM and PVA has certain viscoelastic, resulting in uneven distribution. The addition of SiO<sub>2</sub> increased the biocompatibility and the pore structure of PLCFM, as shown in Fig. 6. With the increase of SiO<sub>2</sub>, the structure of the cell is more regular. This increased the mechanical properties of the material, which is consistent with the test results. It can be seen from Table 1, the mass fraction of Si increased with the addition of SiO<sub>2</sub>, which was mainly distributed in the wall of holes of bubble. When the amount was more than 10%, Si rapidly increased, at this time, most of the silicon atoms are attached to the surface of the bubble hole. Therefore, the PLCFM has better biocompatibility when the SiO<sub>2</sub> content is 10%.

**Table 1.** Concentration of Si in PLCFM with Different SiO<sub>2</sub> Content

SiO <sub>2</sub>	0%	5%	10%	15%	20%
Wt%	2.48	4.31	5.17	11.14	12.46

### Effect of Silica on the Thermal Performance Analysis of PLCFM

#### DSC

The results from the DSC for PLCFM are presented in Fig. 7. According to the compatibility evaluation standard of polymer thermodynamics, the biological compatibility of dissimilar substances is determined using the glass transition temperature ( $T_g$ ) (Wu *et al.* 2014). When fully compatible, the glass transition temperature is combined into one value; however, when the phases are partially compatible, the glass transition temperature shows a heat ladder. As can be seen from Fig. 7., all the PLCFM exhibited a single glass transition temperature, but the PLFM showed a strong endothermic peak at 159 °C, which indicated that the various constituents of PLFM were not fully compatible, suggesting that the addition of silica improved the material's biocompatibility. The pyrolysis endothermic peak at 200 to 250 °C was produced by molecular cracking (Jiao *et al.* 2013). The temperature corresponding to the pyrolysis peak lay along the length of the molecular chain; with decreasing silica content, the tendency to the produce a molecular chain reaction increased, enhancing the intermolecular forces.

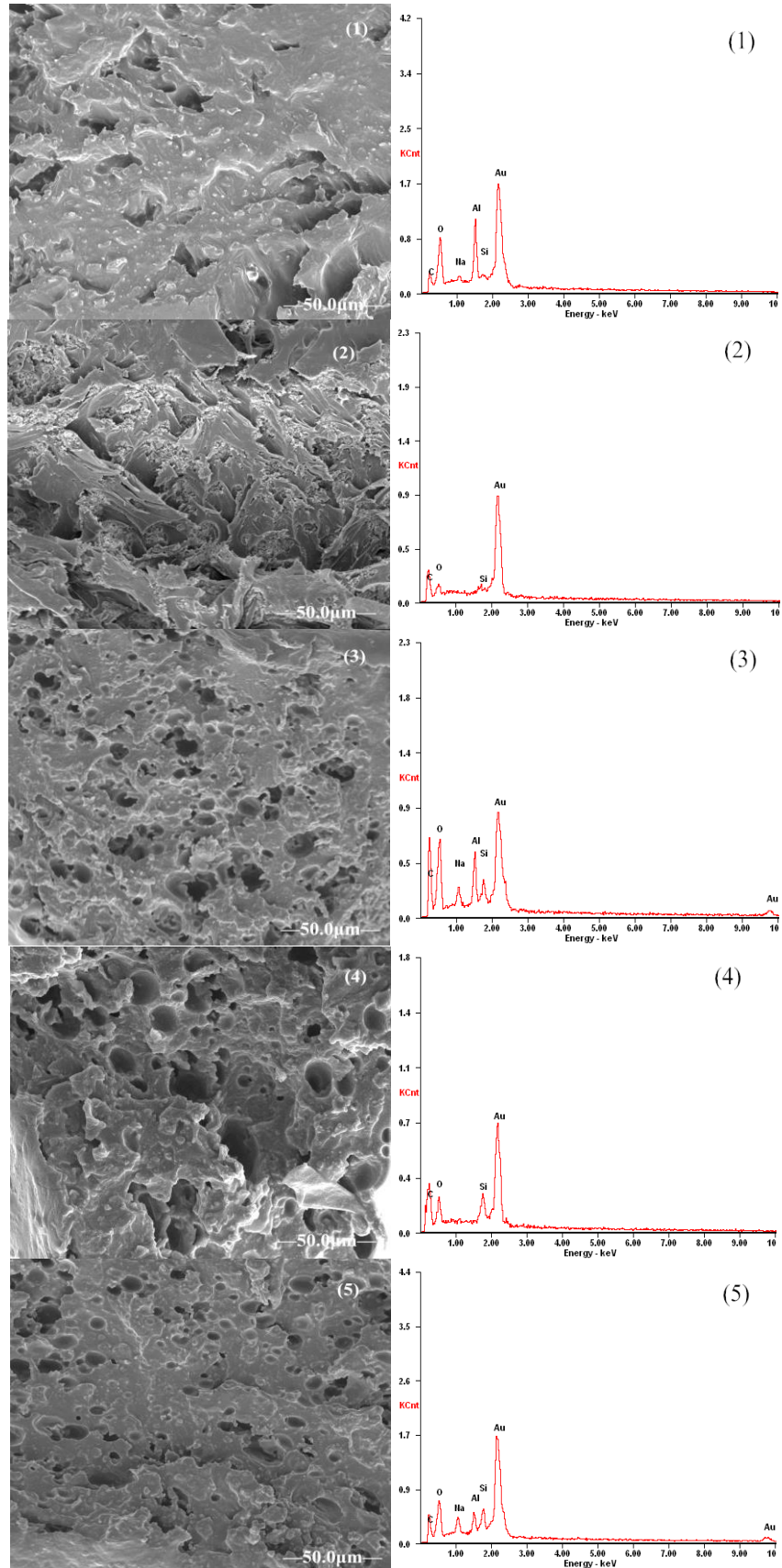


**Fig. 6.** SEM for PLCFM: SiO<sub>2</sub> contents (%) (1)-0; (2)-5; (3)-10; (4)-15; (5)-20

The highest temperature was reached when the silica content was 10%. When the silica content was increased further, the molecular chain lengthened and the energy required for pyrolysis decreased, such that a lower temperature could have induced pyrolysis in the material.

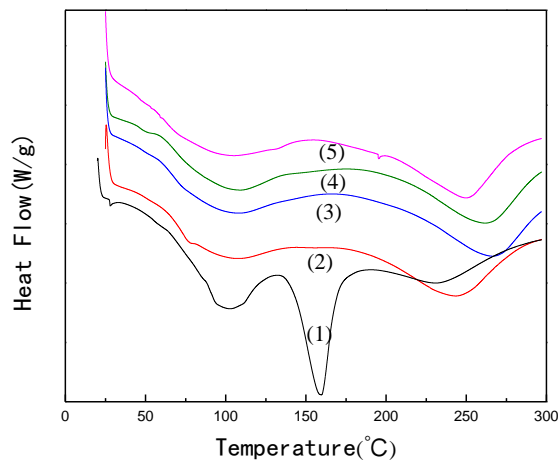


**Fig. 7.** DSC for PLCFM: SiO<sub>2</sub> contents (%) (1)-0; (2)-5; (3)-10; (4)-15; (5)-20

The effects of silica content on the glass transition temperature of the PLCFM are presented in Fig. 8. The  $T_g$  of PLCFM was lower than that of PLFM (90.63 °C) but much higher than that of TEOS, indicating that the compatibility of the two materials were improved by the TEOS, such that the difference between the  $T_g$  of the two phases was reduced. It could be shown using a DSC test that the addition of TEOS caused the PVA and alkali lignin to become bonded together. Under high-speed stirring, the incorporation of lower silica contents had the effect of facilitating a uniform cross-linking between alkali lignin and polyvinyl alcohol. When the amount of silica was increased, the cross-linking was enhanced and the glass transition temperature decreased. The lowest  $T_g$  value, of 64.6 °C, was reached when the silica content added was 10%. When the silica content was further increased beyond this point, the crosslink uniformity declined, leading to uneven heating of PLCFM and a rise in  $T_g$ .

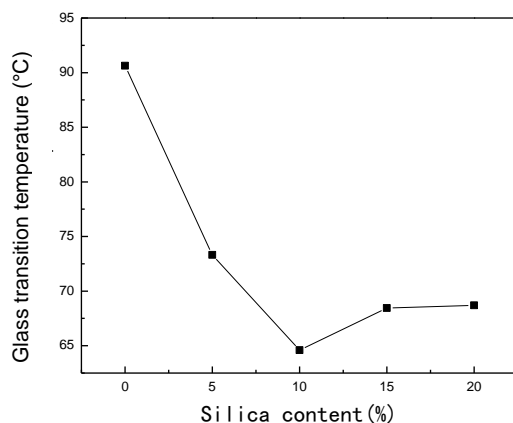


**Fig. 8.** The glass transition temperature of PLCFM with different silica contents

## TGA/DTG

Figure 9 shows the TGA curves of PLCFM with different silica contents. Utilizing silica particles of a smaller size can lead to a denser foam material. Adding silica into the foam material not only improved its strength and toughness, but also greatly improved its water resistance and heat resistance. As can be seen from the graph, the weight loss is divided into three stages. The first stage consists mainly of the volatilization of water and other solvents, including formaldehyde and alcohols (Neil and Weir 2000). With the addition of the silica, the water absorption capacity of the PLCFM was reduced and the moisture content of the PLCFM gradually decreased, causing the weight loss fraction to decrease gradually. Adding a smaller amount of TEOS promoted heat resistant properties. During the second stage, the adjacent hydroxyl reaction caused a decrease in moisture, followed by the formation of an ether bond generated by an acetal reaction, and then lignin began to degrade. The TGA fraction underwent a notable decrease during the second stage, reaching of 60%. The third stage consists of the further degradation of the residual polymer. The TGA fraction underwent smaller changes when the temperature was increased (Hang *et al.* 2011). The residual quantity of the PLCFM was higher than that of PLFM because of the influence of the silica.

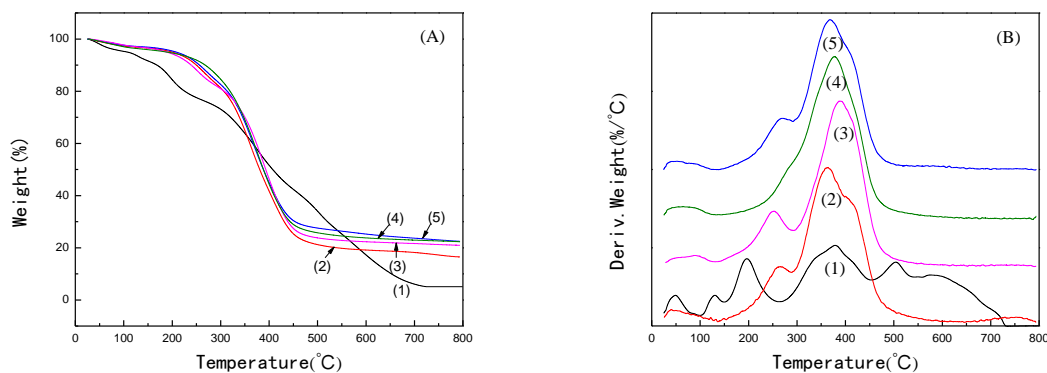


**Fig. 9.** TGA (A)/DTG (B) curves for PLCFM: SiO<sub>2</sub> contents (%) (1)-0; (2)-5; (3)-10; (4)-15; (5)-20

Figure 10 reflects the maximum weight loss rate ( $V_{max}$ ) for the PLCFM and its corresponding temperature ( $T_{Vmax}$ ), which initially increased and then decreased with the increase of silica content. The TGA curve of the PLFM can be seen to be irregular, and the temperature corresponded to the maximum weight loss rate showed deviation because of the poor biological compatibility. The TEOS exhibited good dispersion, was able to closely connect with the PLFM via chemical bonds, and thus could form a better network structure to increase the heat resistance of the material. The lower silica content was propitious to hydrolysis and the polycondensation reaction and facilitated the close connection between the molecules. When the concentration was increased, the maximum degradation temperature increased. PLCFM showed the maximum weight loss temperature when the silica content was 10%. When the silica content was increased further, resistance increased between the molecules, the molecular bonds lost energy when the temperature increased, the temperature corresponding to the maximum weight loss rate decreased.

Changes in weight loss rate primarily depend on the length of chain and the molecular chain growth by cross-linked with formaldehyde; the molecular chain cleavage rate also increases with increasing temperature (Neil and Weir 2000). At the same time,

the TEOS hydrolysis generated a proton, which can make hydroxyls undergo a protonation reaction, thereby accelerating the degradation of PLCFM. The maximum degradation rate increased. When the silica content was 10%, PLCFM reached its maximum degradation rate. When the silica content was further increased, its dispersion and the crosslinking density with PLFM decreased, and the amount of proton produced from silica decreased, leading to a slow protonation reaction, which was not conducive to degradation.

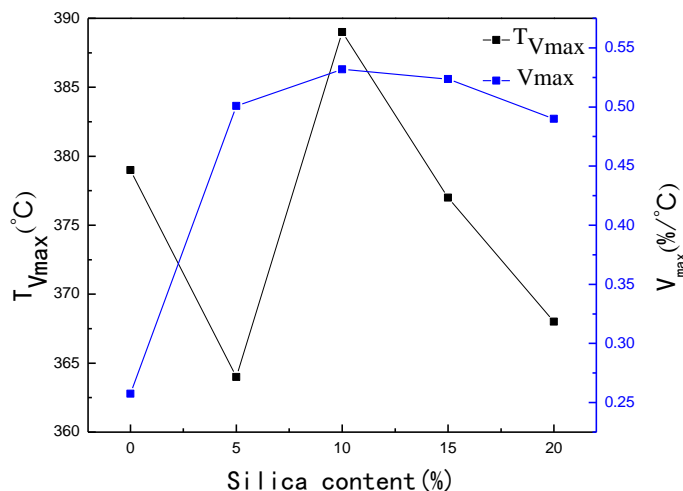


**Fig. 10.** The most rapid weight loss rate ( $V_{max}$ ) and corresponding temperature ( $T_{V_{max}}$ ) for PLCFM

## CONCLUSIONS

1. The addition of the silica notably improved the heat resistance property of the foam material, as the initial decomposition temperature of the material was greatly increased. The PVA exhibited good biocompatibility with silica and alkali lignin, and the melting temperature also increased significantly. When the silica content was 10%, the thermal melting temperature reached 268 °C, which is 110 °C higher than the melting temperature without the addition of silica. At the same time, the addition of silica improved the mechanical properties of the material.
2. The hydrolysate of the TEOS caused a condensation reaction in the hydroxyl in the PLFM, generating a consistent and stable interpenetrating network structure, which, when coupled with the effects of hydrogen bonding, facilitated the linkage of the silica to the PLFM.

## ACKNOWLEDGMENTS

This work was supported by the National Science & Technology Support Program during the Twelfth Five-year Plan Period (2012BAD24B0403), the Science & Technology Supporting Agricultural Field Key Program, Jilin, China (20110269), and this work was financially supported by the Key Projects (20140204006GX) of Science and Technology Department of Jilin Province.

## REFERENCES CITED

- Abdul Khalil, H. P. S., Marliana, M. M., and Alshammari, T. (2011) "Material properties of epoxy-reinforced biocomposites with lignin from empty fruit bunch as curing agent," *BioResources* 6(4), 5206-5223. DOI: 10.15376/biores.6.4.5206-5223
- Anbarasan, R., Pandiarajaguru, R., Prabhu, R., Dhanalakshmi, V., Jayalakshmi, A., Dhanalakshmi, B., Nisha, S. U., Gandhi, S., and Jayalakshmi, T. (2010) "Synthesis, characterizations, and mechanical properties of structurally modified poly (vinyl alcohol)," *Journal of Applied Polymer Science* 117(4), 2059-2068. DOI: 10.1002/app.32033
- Brinker, C. J., Keefer, K. D., and Sehaefer, D. W. (1984). "Sol-gel transition in simple silicates II," *Journal of Non-Crystalline Solids* 63(1-2), 45-59. DOI: 10.1016/0022-3093(84)90385-5
- Corradini, E., Pineda, E. A. G., and Hechenleitner, A. W. (1999). "Lignin-poly (vinyl alcohol) blends studied by thermal analysis," *Polymer Degradation and Stability* 66(2), 199-208. DOI: 10.1016/S0141-3910(99)00066-X
- de Oliveira, A. A. R., Ciminelli, V., Dantas, M. M. S., Mansur, H. S., and Pereira, M. M. (2008). "Acid character control of bioactive glass/polyvinyl alcohol hybrid foams produced sol-gel," *Journal of Sol-gel Science and Technology* 47(3), 335-346. DOI: 10.1007/s10971-008-1777-1
- Hang, Z. S., Tan, L. H., Cao, X. M., Ju, F. Y., Ying, S. J., and Xu, F. M. (2011). "Preparation of melamine microfibers by reaction electrospinning," *Materials Letters* 65(7), 1079-1081. DOI: 10.1016/j.matlet.2011.01.010
- Hsiue, G. H., Kuo, W. J., Huang, Y. P., and Jeng, R. J. (2000) "Microstructural and morphological characteristics of PS-SiO<sub>2</sub> nanocomposites," *Polymer* 41(8), 2813-2825. DOI: 10.1016/S0032-3861(99)00478-4
- Jiao, L. L., Xiao, H. H., Wang, Q. S., and Sun, J. H. (2013). "Thermal degradation characteristics of rigid polyurethane foam and the volatile products analysis with TG-FTIR-MS," *Polymer Degradation and Stability* 98(12), 2687-2696. DOI: 10.1016/j.polymdegradstab.2013.09.032
- Kabir, M. E., Saha, M. C., and Jeelani, S. (2006). "Tensile and fracture behavior of polymer foams," *Materials Science and Engineering A* 429 (1-2), 225-235. DOI: 10.1016/j.msea.2006.05.133
- Lewis, N. G., and Yamamoto, E. (1990). "Lignin: Occurrence, biogenesis and biodegradation," *Annual Review of Plant Physiology and Plant Molecular Biology* 41, 455-496. DOI: 10.1146/annurev.pp.41.060190.002323
- Li, X. L., Li, Y. F., Zhang, S. D., and Ye, Z. F. (2012). "Preparation and characterization of new foam adsorbents of poly(vinyl alcohol)/chitosan composites and their removal for dye and heavy metal from aqueous solution," *Chemical Engineering Journal* 183, 88-97. DOI: 10.1016/j.cej.2011.12.025.
- Light Industry Federation. (2005). "GB/T8810-2005 Determination of water absorption of rigid cellular plastics," *Standards Press, China*.
- Light Industry Federation. (2006). "GB/T 6343-2009/ISO 845:2006 Cellular plastics and rubbers—Determination of apparent density," *Standards Press, China*.
- Luo, H. C., Ren, S. X., Ma, Y. L., and Fang, G.Z. (2015). "Preparation and properties of polyvinyl alcohol-alkali lignin foam material (PLFM)," *Journal of Beijing Forestry University*, 37(4):127-134. DOI: 10.13332/j.1000-1522.20140347.

- Malay, O., Yilgor, I., and Menciloglu, Y. Z. (2013). "Effects of solvent on TEOS hydrolysis kinetics and silica particle size under basic conditions," *Journal of Sol-gel Science and Technology* 67(2), 351-361. DOI: 10.1007/s10971-013-3088-4
- Malutan, T., Nicu, R., and Popa, V. I. (2008). "Contribution to the study of hydroxymetylation reaction of alkali lignin," *BioResources* 3(1), 13-20. DOI: 10.15376/biores.3.1.13-20
- National Plastic Products Standardization Technical Committee. (1991). "GB13022-91 Plastics—Determination of tensile properties of films," *Standards Press, China*.
- Neil, A., and Weir, B. M. (2000). "Retardation of photo-yellowing of lignin-rich pulp," *Polymer Degradation and Stability* 69(1), 121-126. DOI: 10.1016/S0141-3910(00)00049-5
- Pan, X. J., and Saddler, J. N. (2013). "Effect of replacing polyol by organosolv and kraft lignin on the property and structure of rigid polyurethane foam," *Biotechnology for Biofuels* 6, 2-10. DOI: 10.1186/1754-6834-6-12
- Rachipudi, P. S., Kariduraganavar, M. Y., Kittur, A. A., and Sajjan, A. M. (2011). "Synthesis and characterization of sulfonated-poly(vinyl alcohol) membranes for the pervaporation dehydration of isopropanol," *Journal of Membrane Science* 383(1-2), 224-234. DOI: 10.1016/j.memsci.2011.08.040
- Salinas, A. J., Merino, J. M., Baonneau, F., Gil, F. J., and Vallet-Regi, M. (2007). "Microstructure and macroscopic properties of bioactive CaO-SiO<sub>2</sub>-PDMS hybrids," *Journal of Biomedical Materials Research Part B - Applied Biomaterials* 81B(1), 274-282. DOI: 10.1002/jbm.b.30663
- Schmidt, H., Scholze, H., and Kaiser, A. (1984). "Principles of hydrolysis and condensation reaction of alkoxysilanes," *Journal of Non-Crystalline Solids* 63(1-2), 1-11. DOI: 10.1016/0022-3093(84)90381-8
- Su, L., Xing, Z. H., Wang, D., Xu, G. H., Ren, S. X., and Fang, G. Z. (2013). "Mechanical properties research and structural characterization of alkali lignin/poly(vinyl alcohol) reaction films," *BioResources* 8(3), 3532-3543. DOI: 10.15376/biores.8.3.3532-3543
- Wouters, M. E. L., Wolfs, D. P., van der Linda, M. C., Hovens, J. H. P., and Tinnemans, A. H. A. (2004). "Transparent UV curable antistatic hybrid coating on polycarbonate prepared by the sol-gel method," *Progress in Organic Coatings* 51(4), 312-320. DOI: 10.1016/j.porgcoat.2004.07.020
- Wu, L. Y. L., Tan, G. H., Zeng, X. T., Li, T. H., and Chen, Z. (2006). "Synthesis and characterization of transparent hydrophobic sol-gel hard coatings," *Journal of Sol-gel Science and Technology* 38(1), 85-89. DOI: 10.1007/s10971-006-5917-1
- Wu, K., Wang, J. K., Lin, F. Q., Liu, Y. C., Yang, K., Zhou, X., and Zhang, D. Q. (2014). "Modification and characterization of the poly (vinyl chloride)/thermoplastic polyurethane foam composite material," *Polymer Composites* 35(9), 1716-1722. DOI: 10.1002/pc.22825
- Zaharescu, M., Jitianu, A., Braileanu, A., Madarasz, J., Nova, C., and Pokol, G. (2003). "Composition and thermal stability of SiO<sub>2</sub>-based hybrid materials TEOS-MTEOS system," *Journal of Thermal Analysis and Calorimetry* 71(2), 421-428. DOI: 10.1023/A:1022883221776

Article submitted: January 7, 2015; Peer review completed: June 14, 2015; Revised version received: July 21, 2015; Accepted: July 22, 2015; Published: August 3, 2015. DOI: 10.15376/biores.10.3.5961-5973